# High-Speed Deforming Behavior of Cavitation Cloud and Propagation of Bubble Collapse

**Yasuhiro SAITO and Keiichi SATO**

*Department of Mechanical Engineering, Kanazawa Institute of Technology,*
*7-1 Ogigaoka, Nonoichi, Ishikawa, 921-8501*
*y-sugi@neptune.kanazawa-it.ac.jp*

*Corresponding author* **Yasuhiro SAITO**

## Abstract

*It is known that a cavitation cloud causes high impact when it collapses. Pressure waves generated by the cavity collapse propagate into surrounding bubbles and induce them to collapse. The mechanism of the high impact due to the collapse of cavitation clouds and the propagation of bubble collapse is an interesting problem. In this study, we investigate the detailed behaviors of cavitation cloud and the propagation behavior of bubble collapse with an image processing technique. We used two types of observing methods to measure these behaviors. The one was a method using a high-speed video camera for the behaviors of cavitation cloud and the propagation of bubble collapse. The other one was a method using a still instantaneous photograph with a multi-exposure method for detailed and high-resolution observation of rebound behavior of cavitation clouds. As a result, it was shown that there was a tendency toward higher rebounding speed at the earlier stage of the collapse of cavitation cloud. Moreover, it was found that the propagation velocity of bubbles collapse was on the order of several 100 m/s to 1000 m/s.*

**Keyword:** *Cavitation cloud, Propagation of bubble collapse, High-speed video observation, Multi-exposure method, Pressure wave*

## 1. Introduction

It is known that cavitation bubble generates pressure waves or shock waves when it collapses. These pressure waves and impacts cause vibration, noise and erosion in fluid machinery or systems. There have been many studies on the cavitation bubble collapse. Shima et al. [1] showed that the shock wave produced by the collapse of a bubble is generated when the bubble rebounds. Ellis [2] observed experimentally the shock wave produced by ultra-sonic cavities. Miyazaki et al. [3] observed a shock-ring in the experiment of vibratory device. Matsumoto et al. [4] showed the possibility of concentration of shock waves by the numerical analysis of the propagation of shock waves in bubbly flow condition. There have been also some studies on the shock wave interference with bubbles. Field et al. [5] investigated in a series of their studies that the shock waves and the micro-jets cause the chain-reaction of collapse of cavities in gelatin. Recently, Sato et al. [6] showed the phenomena of the chain-reaction behavior (propagating upstream direction) at bubble collapses in the cavitating convergent-divergent nozzle.

In the actual flow field, the cavitation is in the state of the cavitation clouds in most cases. On the flow field in the wake of a circular cylinder, it forms a vortex-type cavitation cloud. There are many experimental and numerical studies of the cavitation cloud which show the high impact of the cavitation cloud [6-12].

Sato et al. have conducted studies of the unsteady state and the high impact of cavitation cloud in a simple flow field. In the wake of a bluff body, some collapsing patterns of cavity and the cavitation impact were studied [9,10,12]. In the case of cloud cavitation in the wake of a convergent-divergent nozzle, the chain-reaction of cavity collapse are observed. In the wake of a circular cylinder, the vortex (cloud) cavitation shows the propagation behavior of cavity when it collapses. And the propagating behavior of the shock-ring is shown in the experiment of vibratory device [6].

The high-speed framing technology develops to higher extent so that it is possible to relate the collapsing behavior of cavitation with its impact [6, 13]. Recently, the high-speed video camera with a

framing rate of 1Mfps was invented [14]. Therefore, we can observe the details of cavitation collapse behavior, and it is necessary to develop the image analysis system.

In this study, we observe the collapsing behaviors of cavitation cloud in the wake of a circular cylinder using a high-speed video camera and a still camera triggered by the cavitation impact. We also observe the pressure waves and propagation of the bubble collapse using an ultra-high-speed video camera. Especially, we try to analyze and estimate quantitatively the collapsing behavior of the vortex cavities and the propagation behaviors of many surrounding small bubbles.

## 2. Experimental apparatus and procedure

The experiments were conducted using a closed-type cavitation tunnel with a rectangular channel. The test section is 60 mm x 80 mm in cross-section as shown in Fig.1. A 30 mm diameter cylinder was installed vertically as a cavitator. A PZT sensor flash-mounted on the inner wall and an accelerometer (Teac, 703FB) installed on the outer surface of a stainless rod were used to measure the cavitation impact [9, 10]. The inner surface of the stainless rod was 3mm in diameter, and the rod was separated from the surrounding wall using silicon rubber. Figure 2 shows the block diagram of measurement system [9]. Two kinds of high-speed video cameras were used to observe cavitation bubbles. The first one with a maximum framing rate of 40.5Kfps (Kodak, EKTAPRO Model 4540) was used in most cavitation experiments. The other one was an ultra-high speed camera with a maximum rate of 1Mfps [14].

Two nano-pulse-lights (Sugawara, NP-1A, flash duration 180ns) were used for a double-exposure method. The test section was uniformly illuminated using these lights with red and blue colors. A deforming behavior of cavity can be measured by resolving one picture taken by a double-exposure method into two pictures. A delay circuit adjusts the flash interval. The error can be evaluated as about 10% from the picture illuminated simultaneously.

The cavitation number σ and Reynolds number Re are defined as follows:

$$\sigma = 2(P-P_v) / \rho U^2 \tag{1}$$
$$Re = U \cdot d / \nu \tag{2}$$

where P and U are static pressure and freestream velocity, respectively. $\rho$, Pv and $\nu$ are the density, vapor pressure and kinematic viscosity of water, respectively. Other important parameters include the temperature Tw, the dissolved content of oxygen in the water β, and the frame speed of a high-speed video camera Fs.

## 3. Experimental results and discussion
### 3.1 High-speed video camera observation

Figure 3 shows cavity behavior taken by the high-speed video camera system at a framing rate of 9000 fps. A picture of Frame No. 0 is an image of detecting the impact. The negative and positive number frames correspond to the images before and after the detection of impact, respectively.

It is observed that cavities shed periodically and move downstream with a rotating motion. This shedding-type cavity divides into some parts near Frame No. -10 and collapses near the solid wall (Frame No. -10 ~ 0). It stays near the solid wall where it collapses intensely and generates high impact. Then the rebound motion of the cavity is observed. This collapsing behavior corresponds to the axial collapse [10, 11] and relates to the occurrence of high impact.
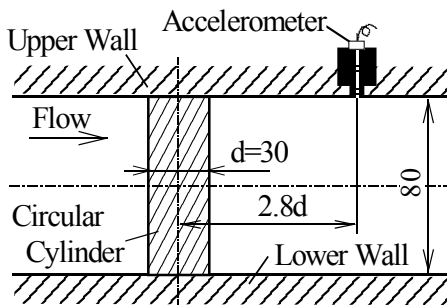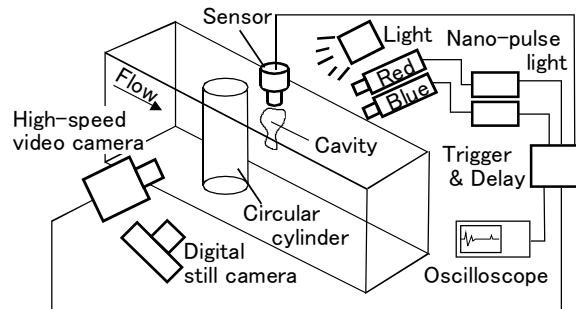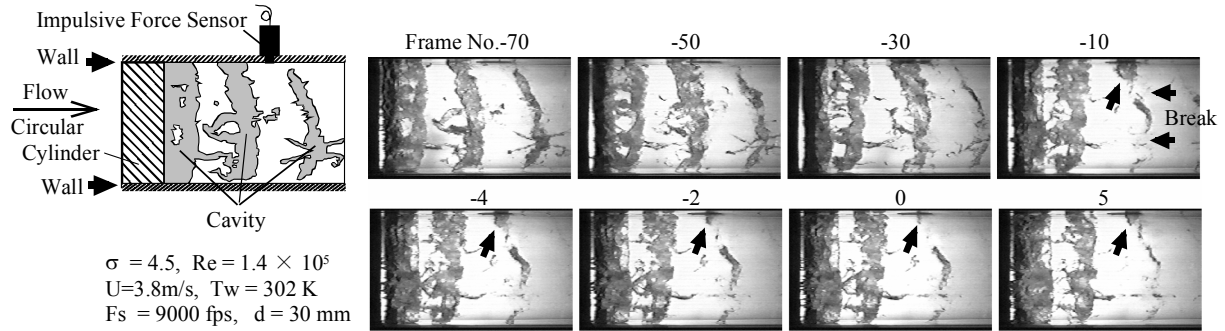


Fig. 1 Test section



Fig.2 Experimental setup

$\sigma = 4.5$, $Re = 1.4 \times 10^5$
U=3.8m/s, Tw = 302 K
Fs = 9000 fps, d = 30 mm

Fig.3 Cavity collapsing behavior in the wake of circular cylinder [12]



(a)Blue image
(delay time 0μs )

(b)Red image
(delay time 150μs )

(c) Waveform of impact and two flashes

$\sigma = 4.7$ $Re = 1.2 \times 10^5$ $\beta = 1.4\text{-}1.6$ mg/$\ell$ d = 30 mm
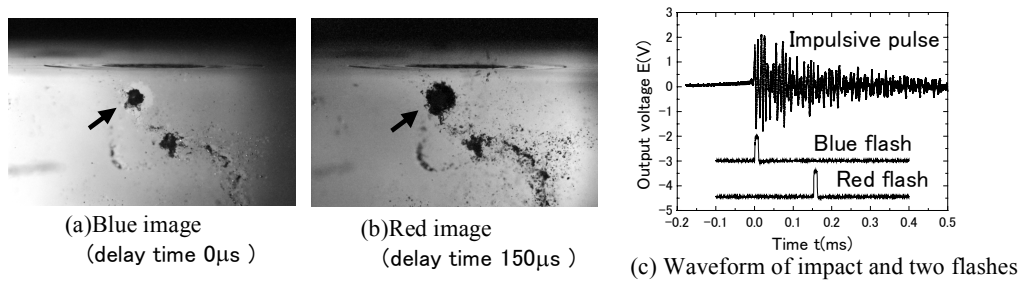
Fig.4 Deformation of rebounded cavity



(a) Change of cavity diameter

(b) Deforming velocity of cavity

$\sigma = 4.7$ $Re = 1.3 \times 10^5$ $\beta = 1.3\text{-}3.6$ mg/$\ell$
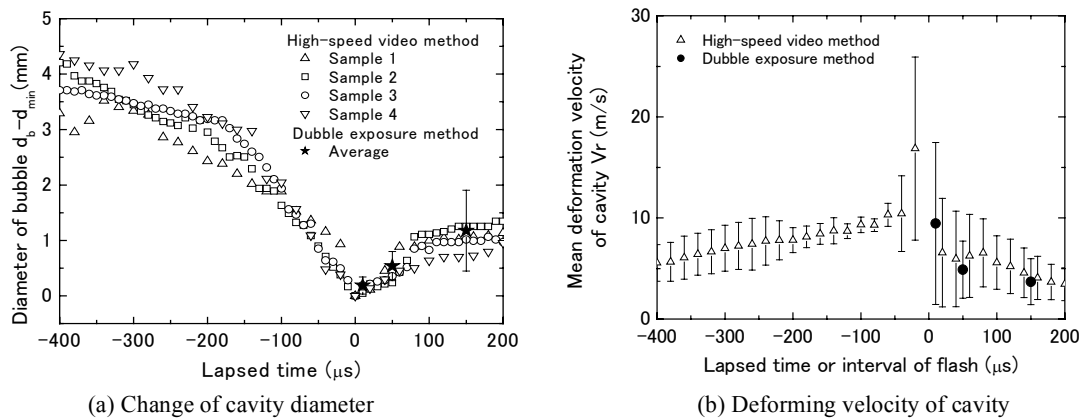
Fig.5 Deforming Behavior of cavity

## 3.2 Measurement of the cavity behavior using a double-exposure method

We examined the cavity behavior using the nano-pulse light and the digital still camera so that the cavity behavior (especially, rebounding behavior) could be observed more clearly. The blue light flashed when the sensor detected the impulsive pulse, then the red one flashed after 0, 10, 50 or 150μs. Here, the light flashed in 5μs after the rising point of the pulse because of the characteristic of the system. The resolution of the picture is 0.016mm per pixel. Figure 4 shows the picture photographed by delaying 150μs. The cavity indicated by arrows in Fig. 4 shows the rebound behavior and it grows with the lapse in time.

Such cavitation deforming behavior was measured. Figure 5 shows the change of the projected equivalent diameter and the deforming velocity obtained from the pictures taken by the high-speed video camera or the double exposure method. The projected area of the cavity is estimated using the binary image. The lapsed time 0 shown in Fig. 5 means the time that a bubble reaches minimum size.

The variation of the cavity is estimated on the basis of the minimum equivalent diameter. In these cases, the error of measurements is about 2 pixels; they are about 160μm in the case of the high-speed video camera method and about 30μm in the case of the double-exposure method respectively.

Figure 5(a) shows the variation of cavity diameter. The deforming variation of the cavity diameter increases with lapse of time to collapse. In the case of the rebound behavior, the results of both methods correspond with each other. Figure 5(b) shows the relation between the mean deforming velocity of the cavity and the delay time. The collapsing velocity of cavity around –400μs to –100μs is estimated to be several meters per second and then it reaches to be on the order of 10~30m/s around the final stage of collapse. The growing velocity of the rebound cavity is estimated to be a decrease with the lapse of time. Since the double-exposure method can be measured with the shorter interval of time than the high-speed video camera, we should make a further study of the final stage of the cavity collapse.

## 4. Propagation of the cavity collapse
### 4.1 Cavity collapsing behavior and propagation of the bubble collapse

The condition of the circumference in the cavity collapse is observed using the ultra-high speed video camera at $5 \times 10^5$ fps. Figure 6 shows a typical result. The number in the figure indicates the lapse of time (μs). Figure 6(a) shows the behavior of the cavity collapse at a distance from a wall and Fig. 6(b) shows the behavior of the cavity collapse with impinging motion to the wall. As shown in Fig. 6(a), the main cavity collapses at a distance from the wall around 92μs and shows rebounding motion around 96 to 110μs. Then, the surrounding small bubbles (A~D in Fig. 6(a)) collapse in sequence (Bubble A collapses around 96μs, B, C and D collapse around 110μs, 122μs and 140μs respectively). Similar behavior is also observed in Fig. 6(b). The main cavity collapses around 96μs near solid wall. Then surrounding bubbles A, B, C and D collapse around 100, 104, 110 and 134μs respectively. This propagation speed of bubbles collapse is measured by an image analysis.

## 4.2 Estimation of propagation behavior of the bubble collapse
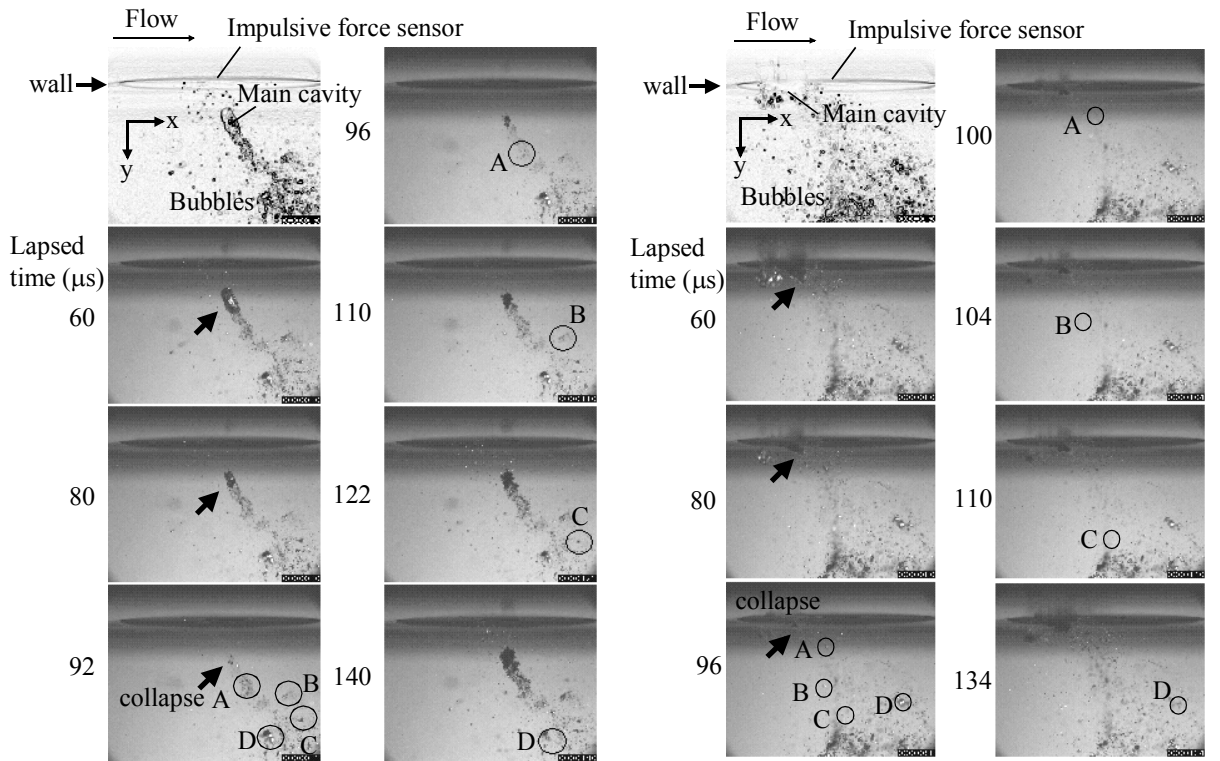


(a)Sample A: Bubble collapse at a distance from solid wall      (b) Sample B: Bubble collapse near solid wall

σ=4.7,   U=3.8 m/s,  Re=1.2x10⁵,  β=0.68mg/ℓ,  Fs= 5 × 10⁵ fps

Fig.6 Propagation behavior of bubble collapse

 Estimation of the propagation behavior is preformed using binary images (312x260 pixels) of each frame. Black pixels, which approximately correspond to bubbles, are counted horizontally (x direction) as shown in Fig. 7. Since the number of black pixels decreases with bubbles collapse, the averaged behavior of bubble collapse (propagation velocity) to the vertical direction (y direction) can be estimated. In this case, however, bubbles scatter spatially and exist at angle with the x-y plane or the y direction. It is approximately estimated that the velocities in y direction given by the analysis roughly evaluate the actual velocities.

### 4.3 Propagation velocity of the bubble collapse
 Figure 8 shows the result of the image analysis of Fig. 6. Figure 8 shows the relation between the
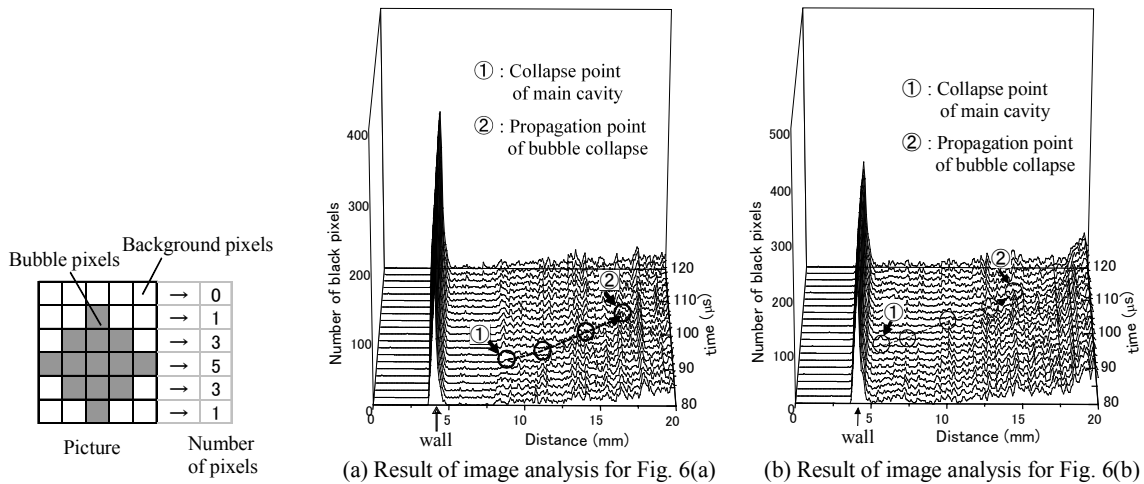


Fig.7 Measurement method

(a) Result of image analysis for Fig. 6(a)  (b) Result of image analysis for Fig. 6(b)

Fig. 8 Result of image analysis



(a) Measured bubbles in Fig. 6(a): Sample A  (b) Measured bubble in Fig. 6(b): Sample B
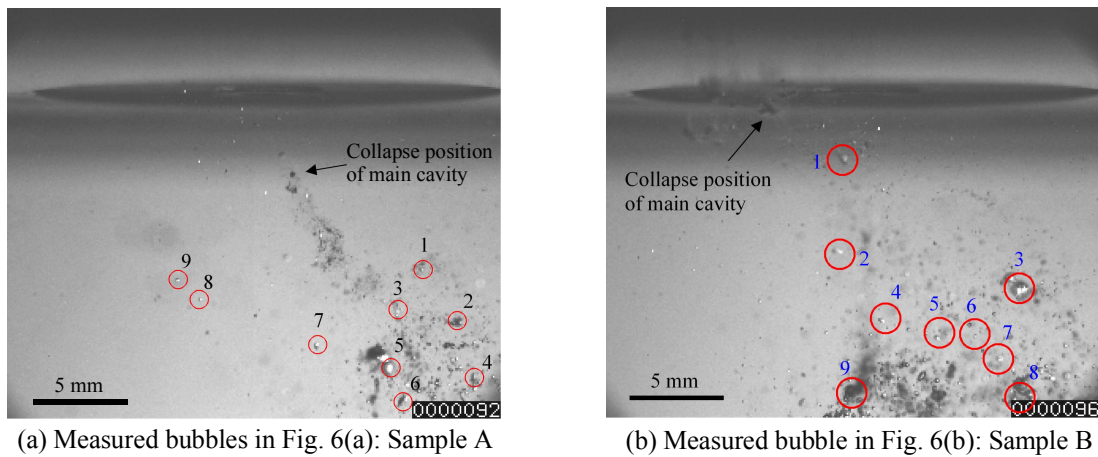
Fig. 9 Cavity aspects at main cavity collapse

Table 1  Data on bubbles measured in Sample A

| Cavity No. | Distance from main cavity collapse point (mm) | Collapse time of bubble t (μs)* | Propagation velocity of bubble collapse Vp (m/s) | Time for bubble collapse tc (μs) | Diameter of bubble $d_b$(mm) |
|---|---|---|---|---|---|
| 1 | 8.6 | 112 | 430 | 8 | 0.34 |
| 2 | 11.8 | 120 | 420 | 14 | 0.67 |
| 3 | 9.3 | 104 | 770 | 6 | 0.65 |
| 4 | 14.5 | 122 | 480 | 12 | 0.46 |
| 5 | 11.6 | 146 | 220 | 32 | 0.89 |
| 6 | 13.5 | 132 | 340 | 26 | 0.59 |
| 7 | 9.2 | 106 | 660 | 10 | 0.37 |
| 8 | 8.3 | 100 | 1040 | 6 | 0.28 |
| 9 | 8.3 | 100 | 1040 | 4 | 0.30 |

∗ Main cavity collapses at 92μs in Fig. 6(a)

Table 2  Data on bubbles measured in Sample B

| Cavity No. | Distance from main cavity collapse point (mm) | Collapse time of bubble t (μs)* | Propagation velocity of bubble collapse Vp (m/s) | Time for bubble collapse tc (μs) | Diameter of bubble $d_b$(mm) |
|---|---|---|---|---|---|
| 1 | 4.9 | 102 | 820 | 8 | 0.61 |
| 2 | 8.5 | 104 | 1060 | 8 | 0.51 |
| 3 | 16.5 | 134 | 440 | 24 | 1.21 |
| 4 | 12.8 | 110 | 910 | 8 | 0.30 |
| 5 | 15.1 | 114 | 840 | 6 | 0.35 |
| 6 | 16.3 | 114 | 910 | 16 | 0.39 |
| 7 | 18.0 | 122 | 690 | 22 | 0.45 |
| 8 | 20.7 | 156 | 340 | – | – |
| 9 | 15.6 | 148 | 300 | – | – |

∗ Main cavity collapses at 96μs in Fig. 6(b)

distance from the top of image and black pixels. The peak on the left hand of the figure corresponds to the wall. Point 1 in the figure shows the collapse point and the time of the main cavity. And Point 2 shows the typical collapse point of the small bubbles (that is a region with small black pixels). It is observed that the collapse of bubbles (the region with small black pixels) moves from Point 1 toward Point 2. The propagation velocity of small bubbles is estimated around 640m/s in the case of Fig. 8(a) and 670m/s in the case of Fig. 8(b) respectively.

Next, each small bubble is estimated from the high-speed video image. Figure 9 indicates some typical small bubbles around the main cavity shown in Fig. 6. Tables 1 and 2 show the velocities measured from the interval of the collapse of the main cavity and the each small bubble. In this case, the bubbles 1~9 in Fig.9 are estimated. As a result, the propagation velocities of bubbles are on the order of 200 to 1000m/s. And the velocity decreases with increase in bubble diameter.

## 5. Conclusion

The behaviors around the cavity collapse and the propagation behaviors of surrounding bubble collapse are observed using the high-speed video camera method and the double-exposure method.
(1) Observation of rebounding behavior of cavities is performed using the double-exposure method. The similar result is also given using the high-speed video camera method.
(2) The deforming velocity of cavity collapse increases near the bubble collapse stage.
(3) The rebounding velocity of the cavity increases immediately after the cavity collapse, then it decrease with the lapse of time.
(4) The bubble collapse propagates into surrounding bubbles through the pressure waves produced by the cavity collapse.
(5) In the present study, the propagation velocity of bubbles is on the order of several hundreds to 1000m/s.

## References

[1] Shima, A., et al., "*An Experimental Study on Effects of a Solid Wall on the Motion of Bubbles and Shock Waves in Bubble Collapse*", Acustica, Vol.48, No.5, (1981), pp.293-301.
[2] Ellis, A.T., "*On jets and shock waves from cavitation*", proc. 6th Symp. Navval Hydrodynamics, Washington, (1966), pp.137-161.
[3] Miyazaki, K., Ahmed, S.M. and Oba, R., "*High-Speed Observations of the Vibratory Cavitation Accompanying Hard Erosion*", JSME Int. J., Ser.B, 36, (1993), pp.511-516.
[4] Kameda, M. and Masumoto, Y., "*Shock Waves in a Liquid Containing Small Gas Bubbles*", Phys. Fluids, vol.8, No.2, (1996), pp.322-335.
[5] Dear, J.P. and Field, J.E., "*A Study of the Collapse of Arrays of Cavities*", J. Fluid Mech., 190(1988), 409-425.
[6] Sato, K., Shimojo, S. and Watanabe, J., "*Observations of Chain-Reaction Behavior at Bubble Collapse Using Ultra High Speed Video Camera*", Cavitation and Multi-Phase Flow Forum, ASME, FEDSM2003, (2003), pp. 1-6.
[7] Knapp, R. T., "*Recent Investigation of the Mechanics of Cavitation and Cavitation Damage*", Trans. ASME, 77(1955), pp.1045-1054.
[8] Shimada, M., et al., "*Influence of the Nuclei Size Distribution on the Collapsing Behavior of the Cloud Cavitation*", JSME International Journal Series B, Vol.43, No.3, (2000), pp.380-385.
[9] Sato, K. and Ogawa, N., "*Collapsing Behavior of Vortex Cavitation Bubbles in the Wake of a Circular Cylinder*", Cavitation and Gas-Liquid Flow in Fluid Machinery Devices, ASME, FED-226, (1995), pp. 119-125.
[10] Sato, K. and Kondo, S., "*Collapsing Behavior of Vortex Cavitation Bubble Near Solid Wall: Spanwise-View Study*", ASME, FED-236, Vol.1, (1996), pp.485-490.
[11] Dominguez-Cortazar, M.A., Franc, J.P. and Michel, J.M., "*The Erosive Axial Collapse of a Cavitating Vortex: An Experimental Study*", Trans. ASME, J. Fluids Eng.,119, (1997), pp. 686-691.
[12] Sato, K., Sugimoto, Y., and Hoshino, K., "*Bubble Collapsing Behavior and Damage Pits of Separated Vortex Cavitation*", Third International Symposium on Cavitation, Grenoble, Vol.2, (1998),   pp. 157-162.
[13] Sato, K., Hachino, K., and Saito, Y., "*Inception and Dynamics of Traveling-Bubble-Type Cavitation in a Venturi*", International Symposium on Cavitation Inception, ASME, FEDSM2003, (2003), pp. 1-8.
[14] Etoh, T.G., et al., "*A CCD Image Sensor of 1Mframes/s for Continuous Image Capturing of 103 Frames*", 2002 Int. Solid-State Circuits Conf., 2.7, (2002), pp.46-47.